Ferrocenium Hexafluorophosphate: Molecular Dynamics in the Solid State

Robert J. Webb,[1] Michael D. Lowery,[2] Yutaka Shiomi,[3] Michio Sorai,[3] Richard J. Wittebort,*[,4] and David N. Hendrickson*[,1]

Department of Chemistry—0506, University of California at San Diego, La Jolla, California 92093-0506, Microcalorimetry Research Center, Faculty of Science, Osaka University, Toyonaka, Osaka 560, Japan, and Department of Chemistry, University of Louisville, Louisville, Kentucky 40292

Received March 25, 1992

The nature of the molecular dynamics associated with the cation of ferrocenium hexafluorophosphate is probed with solid-state ^2H NMR, ^{57}Fe Mösbauer, and single-crystal X-ray diffraction techniques. At room temperature $[Fe(C_5H_5)_2]PF_6$ crystallizes in the monoclinic space group $P2_1/c$ which at 299 K has a = 13.408 (6) Å, b = 9.530 (2) Å, c = 9.482 (2) Å, β = 93.17 (3)°, Z = 4, and d_{calc} = 1.818 g cm^{-3}. Least-squares refinement with 1429 observed reflections led to R = 0.067 and R_w = 0.085. There are two crystallographically independent $[Fe(C_5H_5)_2]^+$ cations. Together with the two 2_1 symmetry-related cations there are four unique orientations of the ferrocenium cations in the solid state at 299 K. Only one orientation of the PF_6^- anion exists at 299 K. When the complex is heated to 360 K, the structure of $[Fe(C_5H_5)_2]PF_6$ changes from the monoclinic room-temperature setting to a cubic setting with a = 6.806 (4) Å, Z = 1, and d_{calc} = 1.743 g cm^{-3}. A unique solution to the structure at 360 K could not be determined due to the uncertainity in Laue symmetry and the limited amount of unique diffraction peaks observable above the diffuse scattering inherent in the plastic phase. However, one possible solution to the structure is presented. Least-squares refinement with 149 observed reflections in $Pm\bar{3}$ led to R = 0.079 and R_w = 0.051. In this space group the structure at 360 K consists of a pseudo-body-centered CsCl-type cubic lattice with orientationally disordered ferrocenium cations and PF_6^- anions. The ferrocenium cations are disordered in four orientations with the C_5 axis at an angle of 18.3° about each of three mutually perpendicular axes to give a total of twelve different orientations at 360 K. The PF_6^- anion is disordered in a total of four orientations, one of which is the orientation seen at 299 K with an occupancy of 0.66 and the other three of which (each with 0.11 occupancy) result from a rotation of the anion from this original orientation by 45° about three mutually perpendicular F–P–F bond axes. Mössbauer spectra recorded from 120 to 375 K for $[Fe(C_5H_5)_2]PF_6$ show that the single quadrupole-split doublet in the spectrum undergoes a dramatic reduction in intensity upon heating the salt from 343 to 355 K. The suggested onset of dynamics associated with the ferrocenium cation is verified and delineated by variable-temperature (185–355 K) ^2H NMR spectra run for a polycrystalline sample of $[Fe(C_5D_5)_2]PF_6$. An axially symmetric powder pattern is seen in the solid-state ^2H NMR spectrum from 188 to 344 K with the residual quadrupole splitting ranging from 67 (2) to 62 (2) kHz, respectively. In this temperature range the $C_5D_5^-$ rings are rotating rapidly about local C_5 axes, and the $[Fe(C_5D_5)_2]^+$ cation at the higher temperatures is also experiencing some small-amplitude libration of its molecular axis. At the 347 K first-order phase transition the 62-kHz residual quadrupole splitting is abruptly and reversibly reduced to essentially zero. The ferrocenium cation is tumbling in the solid as if it were in solution. In order to explain the entropy gain observed by adiabatic calorimetry, a model incorporating correlated motion of the cation and anion which starts at the 347 K phase transition and is present in the high-temperature plastic phase of ferrocenium hexafluorophosphate is developed. As the temperature is increased above the 347 K phase transition, the ferrocenium cation converts from being in four different lattice orientations to a dynamic disorder between twelve orientations. The PF_6^- anion converts from one orientation below 347 K to a dynamic disorder unequally distributed between four orientations above 347 K. An analysis of the crystallographic results shows that $[Fe(C_5H_5)_2]PF_6$ experiences orientational frustration in its plastic high-temperature phase. When the ferrocenium cation is in nine of its twelve available positions above 347 K, the eight nearest PF_6^- anions cannot be in their three low-occupancy sites. On the basis of this model, the entropy gain occurring in the 347 K phase transition is theoretically expected to be $\Delta S = R \ln 5.25$, which compares favorably with the value of $\Delta S = R \ln 5.38$ determined by heat capacity measurements.

Introduction

The conventional view of crystalline materials is one in which the molecular or ionic components exhibit *both* translational and orientational order. However, there is a state of crystalline matter in which the constituents show long-range order but not orientational order. This is the so-called plastic crystalline state.[5] Materials which experience plastic phases are predominantly composed of fairly symmetric polyatomic components that become reorientationally dynamic at some temperature below the melting point. Such materials show unique physical properties which reflect the underlying molecular reorientational motion. For example, substances with plastic phases exhibit solid-state order–disorder phase transitions which are associated with the cooperative onset of molecular dynamics and have transition entropies that exceed the entropy observed upon melting. This is the characteristic thermodynamic signature of plastic crystalline solids which ultimately led to their discovery.[6]

X-ray crystallography of plastic phases also reflects the unique situation of translational order and orientational disorder. Diffraction peaks are observed for such materials mainly due to the translational order present. However, there typically is also a high level of diffuse scattering seen due to the inherent

(1) University of California.
(2) Present address: Department of Chemistry, Stanford University.
(3) Osaka University.
(4) University of Louisville.
(5) Sherwood, J. N. *The Plastically Crystalline State*; John Wiley and Sons: New York, 1979.
(6) Timmermans, J. *J. Phys. Chem. Solids* **1961**, *18*, 1 and references cited within.

0020-1669/92/1331-5211$03.00/0

Table I. Enthalpy and Entropy Arising from the Phase Transitions of Ferrocenium Hexafluorophosphate[a]

phase transition	T_C, K	$\Delta_{trs}H$, kJ/mol	$\Delta_{trs}S$, J/(K mol)
IV–III	210.95		
III–II	213.05	1.95[b]	9.54[b]
II–I	346.94	4.84	13.99

[a] Data from ref 8. [b] The enthalpy and entropy of phase transitions IV–III and III–II are summed to give the tabulated values presented.

orientational disorder. Consequently, only a limited number of diffraction peaks are observable above the unusually large background of diffuse scattering. Structures of plastic crystals are generally found to be cubic even when this is incompatible with the molecular symmetry. For example, *tert*-butyl chloride has a face-centered-cubic (fcc) structure in its plastic phase despite the fact that an isolated molecule has, at most, C_3 rotational symmetry.[7] In this case, the temporally and spatially averaged information obtained from an X-ray analysis of the plastic phase indicates orientational disorder which is totally consistent with the facile dynamic reorientation of the molecular components known to occur in plastic crystals.

Ferrocenium hexafluorophosphate (**1**) is representative of a class of molecular metallocene salts in which the cations and anions are fairly symmetric polyatomic components and are therefore likely to undergo reorientational dynamics and show a crystalline plastic phase. Recently, several experimental observations have hinted that **1** does indeed have a plastic phase. For example, the heat capacity[8] of this solid shows two thermal anomalies, one at roughly 210 K and the other at 347 K (see Table I). The second of these features has a relatively large entropy gain (13.99 J/(mol K) = R ln 5.38) associated with it. In addition, it has been observed that the polarizing colors present for a crystal of **1** below the 347 K phase transition disappear upon going through the transition. This indicates that the structure of **1** is cubic in the high-temperature phase. On the basis of these results, it has been postulated that the ferrocenium cations and hexafluorophosphate anions become reorientationally dynamic at the 347 K phase transition and thus form a plastic phase above 347 K.

The main goal of the present study was to develop a reasonably detailed model of the lattice dynamics which occur in the high-temperature phase of $[Fe(C_5H_5)_2]PF_6$. The technique of solid-state ^2H NMR spectroscopy was examined to see whether it could be used to monitor the dynamics of the paramagnetic cation in the solid-state. While solution-state NMR spectroscopy has long been used to study paramagnetic complexes, it is only recently that high-resolution solid-state studies of paramagnetic complexes have been reported.[9] Recently we showed that ^2H NMR could be used to monitor the onset of dynamics in the solid-state of solvate molecules in paramagnetic mixed-valence iron acetate complexes.[10] It was surprising to find in the present study ^2H NMR signals could readily be seen for deuterons located directly on the ligands in $[Fe(C_5D_5)_2]PF_6$.

Experimental Section

Compound Preparation. Ferrocene (Strem Chemicals) was recrystallized from hexane before use. The perdeuterated ferrocene-d_{10} was prepared according to the method of Fritz and Schäfer.[11] Samples of ferrocenium hexafluorophosphate and ferrocenium-d_{10} hexafluorophosphate were prepared according to a literature method.[12] The resulting dark purple solids were recrystallized from water. Anal. Calcd for ferrocenium hexafluorophosphate ($C_{10}H_{10}FePF_6$): C, 36.27; H, 3.02; Fe, 16.87. Found: C, 36.37; H, 3.03; Fe, 16.72.

Physical Methods. ^{57}Fe Mössbauer measurements were made on a constant-velocity instrument which has been described previously.[13] Mössbauer spectra were least-squares fitted to Lorentzian line shapes with a previously documented computer program.[14] Isomer shift data are reported relative to the isomer shift of iron foil at 300 K but are not corrected for temperature-dependent, second-order Doppler effects.

^2H NMR experiments were performed on a home-built 5.9-T spectrometer described elsewhere.[15,16] The pulse sequence used was a standard quadrupole echo with a pulse width of 2.2 μs and a refocusing delay time, τ, of 30 μs. Chemical shifts for the deuterium spectra are reported relative to D_2O at room temperature. The NMR sample consisted of ~50 mg of microcrystalline $[Fe(C_5D_5)_2]PF_6$ sealed in a Delrin tube ($^1/_4 \times {}^1/_2$ in.).

Powder X-ray diffraction measurements were made on a Rigaku/D-MAX diffraction system, equipped with a copper X-ray tube (λ(CuKα) = 1.5406 Å), a graphite monochromator, and a variable-temperature liquid-nitrogen cold stage. The powder patterns reported are the result of addition of three single scan patterns from 2θ = 10° to 2θ = 45° at 4°/min. The powders were spread evenly in silicone grease on a copper plate. The copper (111) reflection is seen in all of the powder patterns at ca. 2θ = 43.3°.

Single-Crystal X-ray Data Collection and Structure Determination for $[Fe(C_5H_5)_2]PF_6$ (1) at 299 K. Crystals of **1** were grown by slowly cooling a saturated water solution from approximately 50 to 10 °C over a period of 36 h. One of the translucent red/purple crystals, with dimensions of 0.3 × 0.3 × 0.4 mm, was mounted with epoxy on a thin glass fiber and used for data collection. Two shells of data [(2.0° < 2θ < 42.0°) and (42.0° < 2θ < 54°)] were collected (ω scans) on an Enraf-Nonius CAD-4 diffractometer equipped with a molybdenum X-ray tube. The experimentally measured intensities were corrected for Lorentz and polarization effects[17] as well as anomalous dispersion effects.[17] Scattering factors f, $\Delta f'$, and $\Delta f''$ were taken from ref 18. The nonunique data were averaged, and a numerical absorption correction was applied.[17,18] For the absorption correction, the crystal was assumed to be a convex polyhedron bound by plane surfaces, i.e., the crystal faces. A numerical integration of the beam path length was carried out over the entire volume of the sample to evaluate the transmission coefficient for each reflection. The range of transmission factor limits is 0.27–0.55. An extinction correction was made. A summary of data collection parameters is given in Table II.

Systematic absences indicated that the space group of $[Fe(C_5H_5)_2]PF_6$ at 299 K is $P2_1/c$. The structure was solved by heavy-atom methods with the positions of the iron and phosphorus atoms being deduced from a Patterson map. The SHELX-76 computer program for crystal structure determination was used. Subsequent full-matrix, least-squares difference Fourier calculations revealed six fluorine positions and ten disordered carbon positions. In the final cycle, iron atoms were constrained to inversion centers and refined with anisotropic thermal parameters. The phosphorus and fluorine atom positions were independently refined with anisotropic thermal parameters. Carbon atoms were constrained to "ideal" five-membered rings [d(C–C) = 1.42 Å] and an isotropic thermal coefficient was refined for each carbon site. Hydrogen atoms were included as fixed contributors in idealized positions [d(C–H) = 0.96 Å],

(7) Rudman, R.; Post, B. *Mol. Cryst.* **1968**, *5*, 95.
(8) Sorai, M.; Shiomi, Y. *Thermochim. Acta* **1986**, *109*, 29.
(9) (a) Haw, J. F.; Campbell, G. C. *J. Magn. Reson.* **1986**, *66*, 558. (b) Campbell, G. C.; Crosby, R. C.; Haw, J. F. *J. Magn. Reson.* **1986**, *69*, 191. (c) Chacko, V. P.; Granapathy, S.; Bryant, R. G. *J. Am. Chem. Soc.* **1983**, *105*, 5491. (d) Granapathy, S.; Chacko, V. P.; Bryant, R. G.; Etter, M. C. *J. Am. Chem. Soc.* **1986**, *108*, 3159. (e) Granapathy, S.; Bryant, R. G. *J. Magn. Reson.* **1986**, *70*, 149.
(10) (a) Oh, S. M.; Kambara, T.; Hendrickson, D. N.; Sorai, M.; Kaji, K.; Woehler, S. E.; Wittebort, R. J. *J. Am. Chem. Soc.* **1985**, *107*, 5541. (b) Woehler, S. E.; Wittebort, R. J.; Oh, S. M.; Hendrickson, D. N.; Inniss, D.; Strouse, C. E. *J. Am. Chem. Soc.* **1986**, *108*, 2938. (c) Woehler, S. E.; Wittebort, R. J.; Oh, S. M.; Kambara, T.; Hendrickson, D. N.; Inniss, D.; Strouse, C. E. *J. Am. Chem. Soc.* **1987**, *109*, 1063. (d) Oh, S. M.; Wilson, S. R.; Hendrickson, D. N.; Woehler, S. E.; Wittebort, R. J.; Inniss, D.; Strouse, C. E. *J. Am. Chem. Soc.* **1987**, *109*, 1073.
(11) Fritz, H. P.; Schäfer, L. *Chem. Ber.* **1964**, *97*, 1829.
(12) Moore, M. F.; Wilson, S. R.; Cohn, M. J.; Dong, T.-Y.; Mueller-Westerhoff, U. T.; Hendrickson, D. N. *Inorg. Chem.* **1985**, *24*, 4559.
(13) Cohn, M. J.; Timken, M. D.; Hendrickson, D. N. *J. Am. Chem. Soc.* **1984**, *106*, 6683.
(14) Chrisman, B. L.; Tumolillo, T. A. *Comput. Phys. Commun.* **1971**, *2*, 322.
(15) Wittebort, R. J.; Subramanian, R.; Kulshreshtha, N. P.; DuPre, D. B. *J. Chem. Phys.* **1985**, *83*, 2457.
(16) Wittebort, R. J.; Woehler, S. E.; Bradley, C. H. *J. Magn. Reson.* **1986**, *67*, 143.
(17) Stout, G. H.; Jensen, J. H. *X-ray Structure Determination, a Practical Guide*; Macmillan: New York, 1968; see also references therein.
(18) Ibers, J. A., Hamilton, W. C., Eds. *International Tables for X-ray Crystallography*; Kynoch Press: Birmingham, England, 1974; Vol. IV.

Table II. Crystallographic Data for $[Fe(C_5H_5)_2]PF_6$[a]

Structure at 299 K	
chem formula $FeC_{10}H_{10}PF_6$	fw 331.00
a = 13.408 (6) Å	space group $P2_1/c$
b = 9.530 (2) Å	T = 299 K
c = 9.482 (2) Å	λ = 0.710 73 Å
β = 93.17 (3)°	ρ_{calcd} = 1.818 g cm^{-3}
V = 12.09 (1) Å^3	μ = 14.28 cm^{-1}
Z = 4	R = 0.067
	R_w = 0.085
Structure at 360 K	
chem formula $FeC_{10}H_{10}PF_6$	fw 331.00
a = 6.806 (4) Å	λ = 0.710 73 Å
V = 315.3 (3) Å^3	ρ_{calcd} = 1.743 g cm^{-3}
Z = 1	μ = 13.69 cm^{-1}
space group $Pm\bar{3}$	R = 0.079
T = 360 K	R_w = 0.051

[a] $R = \sum||F_o| - |F_c||/\sum|F_o|$; $R_w = [\sum w(|F_o| - |F_c|)^2/\sum w(F_o)^2]^{1/2}$; $w = k/[[\sigma(F_o)]^2 + (pF_o)^2]$.

Table III. Fractional Coordinates for $[Fe(C_5H_5)_2]PF_6$ at 299 K[a]

atom	x/a	y/b	z/c	U_{iso},[b] Å^2
Fe1	0.5	0.0	0.0	0.0401 (7)
Fe2	0.0	0.0	0.0	0.0401 (7)
P	0.2370 (2)[a]	−0.0355 (3)	0.4640 (2)	0.071 (1)
F1	0.2446 (6)	−0.1544 (7)	0.3512 (7)	0.221 (7)
F2	0.2308 (4)	0.0841 (6)	0.5765 (6)	0.136 (5)
F3	0.3544 (4)	−0.0246 (7)	0.4804 (8)	0.090 (4)
F4	0.1221 (5)	−0.0416 (1)	0.4478 (9)	0.071 (4)
F5	0.2372 (5)	−0.1457 (6)	0.5855 (6)	0.181 (6)
F6	0.2370 (6)	0.0787 (8)	0.3440 (7)	0.196 (7)
centroid 1A	0.4722 (7)	0.117 (8)	−0.1349 (21)	
C1A	0.5580	0.1508	−0.1322	0.08 (1)
C2A	0.5180	0.0327	−0.2070	0.089 (7)
C3A	0.4148	0.0238	−0.1823	0.078 (6)
C4A	0.3909	0.1364	−0.0921	0.053 (5)
C5A	0.4794	0.2149	−0.0611	0.073 (6)
centroid 1B	0.5304 (7)	−0.1315 (18)	0.1171 (17)	
C1B	0.4445	−0.1252	0.1491	0.062 (9)
C2B	0.5224	−0.0554	0.2176	0.066 (5)
C3B	0.6114	−0.0809	0.1472	0.058 (5)
C4B	0.5884	−0.1765	0.0351	0.078 (6)
C5B	0.4853	−0.2100	0.0363	0.093 (8)
centroid 2A	−0.1038 (6)	−0.0631 (10)	0.0698 (11)	
C6A	−0.1546	0.0129	−0.0066	0.061 (3)
C7A	−0.1254	−0.1264	−0.0380	0.058 (3)
C8A	−0.0665	−0.1783	0.0796	0.074 (4)
C9A	−0.0592	−0.0711	0.1837	0.071 (4)
C10A	−0.1137	0.0471	0.1304	0.071 (4)
centroid 2B	0.0971 (18)	0.0736 (37)	−0.0804 (18)	
C6B	0.1449	0.0737	0.0314	0.051 (8)
C7B	0.0805	0.1824	−0.0206	0.08 (1)
C8B	0.0391	0.1408	−0.1552	0.07 (1)
C9B	0.0779	0.0064	−0.1864	0.042 (7)
C10B	0.1433	−0.0351	−0.0711	0.08 (1)

[a] Estimated standard deviations in the least significant digits are given in parentheses. Carbon atoms were constrained to "ideal" cyclopentadienyl geometry (d_{C-C} = 1.42 Å), and site occupancy factors for the "A" rings converged to 0.50 (2) and 0.74 (2) for Fe1 and Fe2, respectively. [b] The isotropic temperature factor U_{iso} is expressed as $\exp\{-[(\sin\theta)/\lambda]^2/8\pi^2\}$.

and a group isotropic thermal parameter was refined for them. Successful convergence was indicated by the maximum shift/error for the last cycle. The refinement converged to residuals of R = 0.067 and R_w = 0.085. The final difference Fourier map had no significant features. A final analysis of variance between observed and calculated structure factors showed a slight dependence on $\sin\theta$. Tables III and IV list the positional parameters and selected band distances and angles, respectively, for the 299 K structure of $[Fe(C_5H_5)_2]PF_6$.

A second model utilizing anisotropic thermal parameters for "ordered" carbon atoms converged to lower residuals; however a subsequent Fourier analysis showed considerable electron density between ring carbon atoms and some C–C bond distances that were more than 10σ away from the expected value. For these reasons, this second model was abandoned in favor of the one presented above.

Single-Crystal X-ray Data Collection for $[Fe(C_5H_5)_2]PF_6$ at 360 K. A second translucent red/purple crystal (0.2 × 0.2 × 0.5 mm) was selected from the same batch and mounted on a glass fiber. The space group and cell constants of the crystal used in the high-temperature data collection were checked at 299 K before heating in order to ensure identical crystal morphologies. The crystal was rotated in a stream of nitrogen gas while the temperature of the stream was increased from 26 to 60 °C at a rate of 1.25 °C/min and from 60 to 87 °C at a rate of 0.5 °C/min. The crystal was maintained at 87 °C for 1 h before any measurements were made. Lattice constants were determined at 87 °C and confirmed photographically. Data were collected in four shells with $2\theta < 54°$ for $(\pm h,\pm k,l)$. There were no systematic absences. The intensities were corrected for Lorentz and polarization effects.[17] The data collection parameters are given in Table II.

A unique solution to the structure of **1** at 360 K could not be arrived at due to an uncertainty in the Laue symmetry of the lattice and the large amount of disorder present in phase I (vide infra). Nevertheless, several solutions to the structure were explored in the various possible space group settings. We have chosen to describe just one of these possible settings below, $Pm\bar{3}$ (No. 200). It should be noted that other solutions, most notably the $Pm\bar{3}m$ (No. 221) space group setting, describe the structure at 360 K equally well. Thus the choice of the $Pm\bar{3}$ was arbitrary and does *not* represent a unique solution to the structure of **1** above 347 K.

The structure of **1** at 360 K is cubic and was solved in the space group $Pm\bar{3}$. The nonunique data were averaged, and a numerical absorption correction was applied.[17,18] A symmetry of $m\bar{3}$ was imposed on the iron and phosphorus atoms. A weighted difference Fourier synthesis gave positions for two independent fluorine atoms (suggesting 18 disordered fluorine positions for each phosphorus) and three independent carbon atoms (suggesting 24 disordered cyclopentadienyl ring positions for each iron). The limited amount of unique data in the $Pm\bar{3}$ setting (149 reflections) severely limited the complexity of the disorder model that could be considered. The cyclopentadienyl rings, including the hydrogen atoms, were refined as "idealized" groups [d(C–C) = 1.42 Å and d(C–H) = 0.96 Å]. A single isotropic thermal parameter was refined for each element. The site occupancy factors for the two distinct fluorine positions were found to be 0.195 (2) and 0.055 (2) for F_a and F_b, respectively. The refinement converged to residuals of R = 0.079 and R_w = 0.051 for 18 variables. Successful convergence was indicated by maximum shift/error of 0.001 for the last cycle. The two highest peaks in the final difference Fourier map, 1.46 and 0.36 e/Å^3, were nearly coincident with the iron and phosphorus atoms. A final analysis of variance between observed and calculated structure factors showed a slight dependence on the structure factor amplitude and an inverse dependence on $\sin\theta$. Table II contains the details of the 360 K $Pm\bar{3}$ structure, while Table V lists the positional parameters for this structure.

Table IV. Bond Distances and Angles for $[Fe(C_5H_5)_2]PF_6$ at 299 K[a]

Distances, Å			
P–F1	1.565 (7)	P–F2	1.566 (6)
P–F3	1.577 (7)	P–F4	1.541 (7)
P–F5	1.559 (6)	P–F6	1.575 (7)
Fe1–R1A	1.69 (2)	Fe1–R1B	1.71 (2)
Angles			
R1A–Fe1–R1B	171.3 (8)	R2A–Fe2–R2B	174.4 (10)
F1–P–F2	179.2 (4)	F1–P–F3	90.7 (4)
F1–P–F4	90.4 (5)	F1–P–F5	92.1 (4)
F1–P–F6	90.2 (4)	F2–P–F3	88.5 (3)
F2–P–F4	90.3 (4)	F2–P–F5	89.2 (3)
F2–P–F6	89.5 (4)	F3–P–F4	178.4 (4)
F3–P–F5	90.6 (4)	F3–P–F6	89.1 (4)
F4–P–F5	90.5 (4)	F4–P–F6	89.7 (4)
F5–P–F6	178.6 (4)		

[a] Estimated standard deviations in the least significant digits are given in parentheses. The symbols R1A, R1B, R2A, and R2B represent cyclopentadienyl ring centroids for Fe1 and Fe2.

Results and Discussion

Thermodynamic Results. The results of adiabatic heat capacity measurements for ferrocenium hexafluorophosphate have been previously communicated.[8] The transition temperatures, enthalpy changes, and entropies for the first-order transitions of this compound are summarized in Table I. The present study focuses on the onset of lattice dynamics which occur at the 346.94 K

Table V. Fractional Coordinates for $[Fe(C_5H_5)_2]PF_6$ at 360 K[a]

atom	x/a	y/b	z/c	U_{iso},[b] Å²
P	0.5	0.5	0.5	0.175 (2)
F_a	0.5	0.5	0.2666 (8)	0.185 (3)
F_b	0.331 (4)	0.337 (4)	0.5	0.185 (3)
Fe	0.0	0.0	0.0	0.0953 (10)
centroid	0.047 (3)	-0.066 (3)	0.233 (2)	
C1	-0.1069	0.0023	0.2901	0.118 (5)
C2	0.0751	0.1036	0.2790	0.118 (5)
C3	0.2182	-0.0289	0.2048	0.118 (5)
C4	0.1246	-0.2121	0.1700	0.118 (5)
C5	-0.0764	-0.1928	0.2228	0.118 (5)

[a] Estimated standard deviations in the least significant digits are given in parentheses. Carbon atoms are constrained to "ideal" cyclopentadienyl geometry (d_{C-C} = 1.42 Å). [b] The isotropic temperature factor U_{iso} is expressed as $\exp\{-[(\sin\theta)/\lambda]^2/8\pi^2\}$.

first-order phase transition, for which the associated entropy gain is 13.99 J/(mol K) (=R ln 5.38).

Single-Crystal Structure at 299 K. The single-crystal X-ray structure of $[Fe(C_5H_5)_2]PF_6$ was determined at 299 K. The details of the structure determination, fractional coordinates, and selected bond distances and angles are collected in Tables II–IV, respectively. Compound **1** crystallizes in the monoclinic space group $P2_1/c$ with four formula units per unit cell at 299 K. The asymmetric unit contains two half-cations with the iron atoms sitting on crystallographically imposed centers of inversion, as well as a phosphorus and six fluorine atoms. The average iron to carbon distance in the cation is 2.078 Å, which is typical of that found in other ferrocenium salts (2.075 Å)[19] and somewhat larger than the value found in ferrocene itself (2.045 Å).[20] The average distance from the iron to the cyclopentadienyl, Cp, ring centroid is 1.691 Å. The Cp rings are rotationally disordered as determined by the refinement. This disorder is dynamic as determined by the ^2H NMR data (vide infra). There are two crystallographically independent ferrocenium cations in the asymmetric unit, each of which have another cation in the unit cell related to it by 2_1 symmetry.

A stereoview of the 299 K unit cell is given in Figure 1 with the proposed $Pm\bar{3}$ high-temperature unit cell (vide infra) outlined. The PF_6^- anions in the 299 K structure exhibit nearly octahedral site symmetry with the weighted mean P–F bond length of 1.564 Å, which compares well with the expected value of 1.56 Å.[21] Only one orientation of the PF_6^- anion is apparent in the 299 K structure determination.

Single-Crystal X-ray Structure at 360 K. Single-crystal X-ray diffraction of plastic crystals is beset by several formidable problems.[5] The problems all stem from the orientational disorder inherent in a plastic phase. Crystalline plastic phases typically exhibit cubic structures for which the number of unique diffraction peaks is extremely limited. Compounding this is the extensive diffuse scattering present caused by the orientational disorder. Only the most intense peaks are discernible above the unusually large background of diffuse scattering. For these reasons, the analysis of the crystallographic data collected at 360 K for $[Fe(C_5H_5)_2]PF_6$ was found to be quite difficult.

The solution of the structure of compound **1** in its high-temperature plastic phase was further complicated by Laue group ambiguity. The structure of **1** changes from monoclinic to cubic at the 347 K phase change. The two possible Laue groups for the structure are $m3$ and $m3m$, which differ by a diagonal mirror plane. Even though a full sphere of data was collected, an absolute distinction between $m3$ and $m3m$ could not be made. Therefore, structures in several of the possible space groups were explored. The results presented below are for the $Pm\bar{3}$ (No. 200) refinement of the 360 K structure of **1**. It is important to note the equally good results were obtained for a refinement of $Pm\bar{3}m$ (No. 221).

The average iron to carbon and iron to Cp ring centroid distances in the ferrocenium cation at 360 K are 2.07 and 1.68 Å, respectively. The average P–F bond length in the anion is 1.59 Å. Idealized, rotationally disordered Cp rings, with hydrogen atoms attached, were used in the refinement.

A partial packing diagram of $[Fe(C_5H_5)_2]PF_6$ at 360 K which illustrates the disorder in the ferrocenium cation and PF_6^- anion is shown in Figure 2. The structure consists of a pseudo-body-centered CsCl type cubic lattice with orientationally disordered ferrocenium cations and PF_6^- anions. The ferrocenium cations are disordered in four orientations at an angle of 18.3° about each of three mutually perpendicular axes, giving a total of twelve disordered orientations in the 360 K structure.

The PF_6^- anion is disordered in a total of four orientations at 360 K, one of which is the original orientation seen at 299 K and the other three of which are achieved by rotation of the PF_6^- anion in the original orientation by 45° around three mutually perpendicular F–P–F bond axes. From an examination of the electron density at each fluorine site, it is clear that the four orientations are not populated equally. The refinement model indicates that the PF_6^- anion spends 66% of its total time in the original orientation, while it spends 11% of its time in each of the other three orientations.

Powder X-ray Diffraction. Variable-temperature powder X-ray diffraction (XRD) patterns collected for ferrocenium hexafluorophosphate are shown in Figure 3. The three distinct phases are apparent. Phase I ($T > 347$ K) is cubic. In fact, the positions and intensities of the lines in the 360 K pattern indicate a body-centered lattice with a unit cell dimension of 6.810 Å. This compares well with the results of the 360 K single-crystal structure determination which gave a cell constant of 6.806 Å. Phase II (347 K > T > 210 K) is monoclinic with a space group of $P2_1/c$ as determined from the single-crystal structure described above. The powder XRD data indicate that a third structural phase exists below the low-temperature phase transition at 210 K. Preliminary single-crystal X-ray data were collected at 140 K. It was found that at 140 K the space group of **1** is $P2_1/c$. However, the crystal b axis in the 140 K $P2_1/c$ phase is almost twice that of the b axis in the 299 K $P2_1/c$ phase; i.e., phase II and III are distinct phases with different unit cell parameters but the same space group. The changes in the XRD patterns from 173 to 299 K and from 299 to 360 K are consistent with the single-crystal results.

^{57}Fe Mössbauer Spectroscopy. ^{57}Fe Mössbauer spectra of **1** were recorded at various temperatures in the range 120–375 K. Each spectrum was fit to Lorentzian line shapes via a computer program.[14] The resulting spectral parameters are collected in Table VI, while representative spectra of **1** are shown in Figure 4.

Unlike the large quadrupole splitting (ΔE_Q = 2.4 mm/s) seen in the ^{57}Fe Mössbauer spectrum of ferrocene,[22-25] the spectra of ferrocenium salts typically show a doublet with exceedingly small quadrupole splitting ($\Delta E_Q \simeq 0.1$–0.6 mm/s).[23,24] The quadrupole splitting seen for **1** at 295 K is 0.0103 mm/s and therefore unresolved in the spectrum shown in Figure 4. The isomer shift values (δ) of **1** reported in Table VI are also typical of Fe^{III} metallocenes, generally being 0.1–0.2 mm/s less positive than the value observed for ferrocene, 0.542 mm/s.[22] The widths of the two lines comprising the doublet of **1** are appreciably different

(19) Mammano, N. J.; Zalkin, A.; Landers, A.; Rheingold, A. L. *Inorg. Chem.* **1977**, *16*, 297.
(20) Seiler, P.; Dunitz, J. D. *Acta Crystallogr.* **1979**, *B35*, 1068.
(21) (a) Bode, H.; Clausen, H. Z. *Anorg. Allg. Chem.* **1951**, *265*, 229. (b) Bode, H.; Teufer, G. Z. *Anorg. Allg. Chem.* **1952**, *268*, 20. (c) Cox, B. *J. Chem. Soc.* **1956**, 876.
(22) Ernst, R. D.; Wilson, D. R.; Herber, R. H. *J. Am. Chem. Soc.* **1984**, *106*, 1646.
(23) Wertheim, G. K.; Herber, R. H. *J. Chem. Phys.* **1963**, *38*, 2106.
(24) Greenwood, N. N.; Gibb, T. C. *Mössbauer Spectroscopy*; Chapman and Hall: London, 1971.
(25) Gibb, T. C. *Principles of Mössbauer Spectroscopy*; Chapman and Hall: London, 1976.

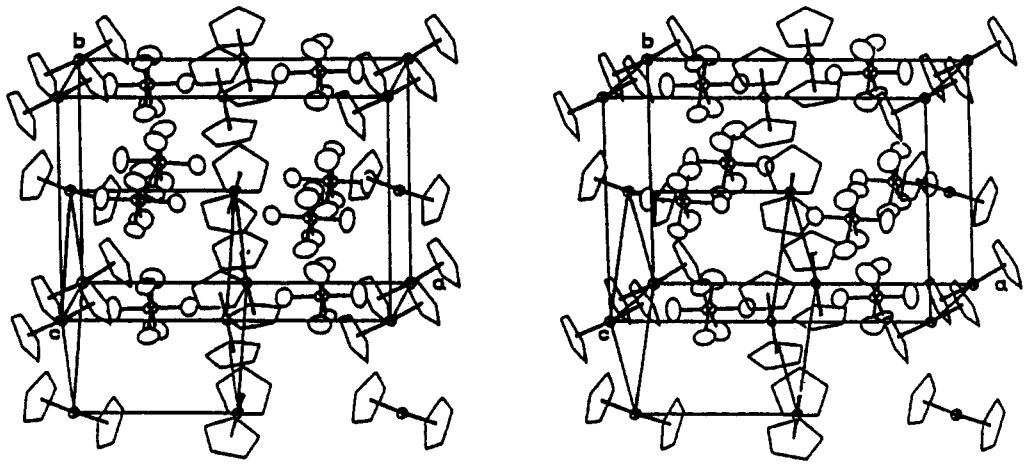

Figure 1. Stereoview of the 299 K $P2_1/c$ unit cell of ferrocenium hexafluorophosphate (**1**). The portion of the 299 K unit cell which becomes the 360 K cubic unit cell is also outlined.

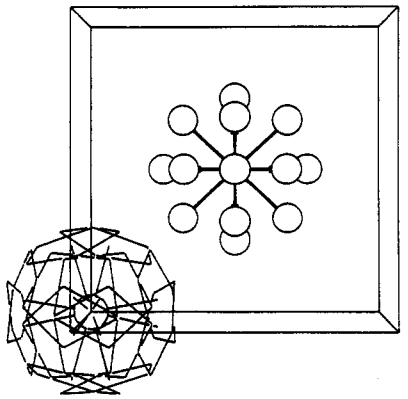

Figure 2. Partial packing diagram of the proposed $Pm\bar{3}$ 360 K cubic structure of $[Fe(C_5H_5)_2]PF_6$. The cation is disordered in twelve orientations, while the PF_6^- anion is disordered in four orientations.

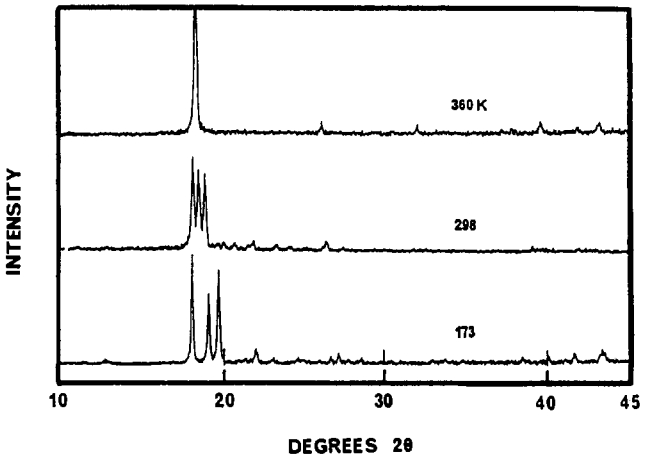

Figure 3. Powder X-ray diffraction pattern for $[Fe(C_5H_5)_2]PF_6$ at various temperatures.

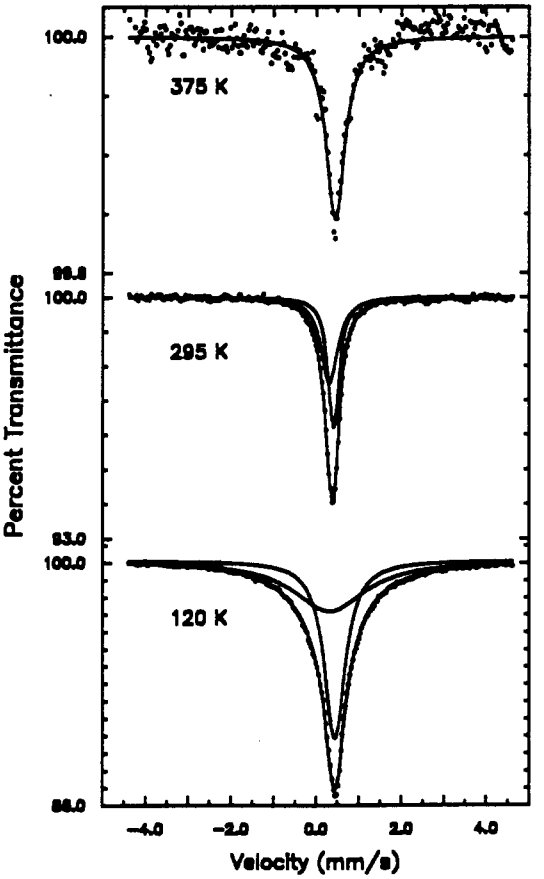

Figure 4. Variable-temperature ^{57}Fe Mössbauer spectra for ferrocenium hexafluorophosphate (**1**).

at lower temperatures. This is likely due to an unequal effect of the rate of paramagnetic relaxation upon the transitions responsible for the two lines. At higher temperatures, the rate of paramagnetic relaxation increases and both nuclear transitions are affected equally.

However, the most significant feature of the spectrum of **1** is the decrease in baseline-normalized area with increasing temperature; see Figure 5. The intensity of a Mössbauer spectrum is related to the probability, f, of zero-phonon (recoilless) events as given in eq 1,[24] where E_γ is the energy of the emitted or absorbed

$$f = \exp(-E_\gamma^2\langle x^2\rangle/(\hbar c)^2) \quad (1)$$

γ-ray, $\langle x^2\rangle$ is some measure of the mean vibrational amplitude of the relevant nucleus in the direction of the γ rays, $\hbar$ is Planck's constant divided by 2π, and c is the speed of light. The precise form of $\langle x^2\rangle$ depends on the vibrational nature of the lattice. In the context of the Debye model of a solid [$N(\omega)$ $\alpha\omega^2$] the form of $\langle x^2\rangle$ transforms eq 1 in the high-temperature limit ($T > {}^1/_2\Theta_D$)[24] into eq 2, where E_R is the recoil energy which for the 14.4-keV

$$f = \exp(-6E_R T/k_B\Theta_D^2) \quad (2)$$

transition of ^{57}Fe is 0.001 95 eV, k_B is Boltzmann's constant, and Θ_D is the Debye temperature of the lattice. A plot of -ln (area) versus temperature is theoretically expected to show a linear behavior in which the slope is related to the Debye temperature.

If, at some temperature, the nature of the solid changes due to a phase transition, there is expected to be a change seen in the

Table VI. ^{57}Fe Mössbauer Fitting Parameters for Ferrocenium Hexafluorophosphate

T, K	ΔE_Q, mm/s	δ^a, mm/s	Γ,^{b} mm/s	−ln (area)^c
120	0.142 (13)^d	0.408 (7)	2.38 (8)	−1.717 (3)
			0.682 (4)	
165	0.162 (14)	0.399 (7)	1.30 (6)	−1.359 (4)
			0.560 (6)	
175	0.137 (6)	0.410 (3)	1.202 (20)	−1.279 (7)
			0.532 (2)	
185	0.145 (9)	0.408 (5)	1.12 (3)	−1.206 (4)
			0.520 (4)	
195	0.165 (12)	0.404 (6)	1.03 (3)	−1.123 (4)
			0.494 (6)	
205	0.219 (16)	0.414 (8)	0.88 (4)	−0.958 (5)
			0.460 (10)	
215	0.146 (11)	0.410 (6)	0.83 (3)	−0.874 (6)
			0.436 (6)	
225	0.217 (13)	0.418 (7)	0.77 (3)	−0.787 (7)
			0.438 (8)	
235	0.128 (5)	0.416 (3)	0.674 (12)	−0.688 (5)
			0.414 (4)	
245	0.133 (9)	0.429 (5)	0.762 (22)	−0.589 (6)
			0.426 (6)	
255	0.126 (7)	0.428 (4)	0.716 (16)	−0.478 (4)
			0.412 (4)	
265	0.115 (8)	0.433 (4)	0.702 (20)	−0.386 (5)
			0.412 (6)	
275	0.108 (9)	0.438 (5)	0.694 (20)	−0.278 (7)
			0.414 (6)	
285	0.116 (10)	0.439 (5)	0.644 (20)	−0.144 (6)
			0.388 (6)	
295	0.103 (8)	0.441 (4)	0.646 (18)	−0.072 (5)
			0.386 (6)	
305	0.084 (11)	0.448 (6)	0.4652 (17)	0.056 (6)
			0.349 (8)	
315	0.124 (12)	0.458 (6)	0.456 (17)	0.197 (8)
			0.373 (10)	
325	0.104 (16)	0.457 (8)	0.469 (23)	0.332 (8)
			0.368 (12)	
335	0.142 (20)	0.469 (10)	0.507 (24)	0.448 (10)
			0.478 (21)	
343		0.451 (31)	0.503 (9)	0.76 (18)
355		0.468 (39)	0.82 (10)	2.38 (25)
375		0.443 (20)	0.58 (5)	2.53 (25)

^{a} Isomer shift relative to iron foil at 300 K. ^{b} Full width at half-height taken from least-squares-fitting program. ^{c} Negative natural logarithm of the normalized spectral area. ^{d} Estimated standard deviations in the least significant digits are given in parentheses.

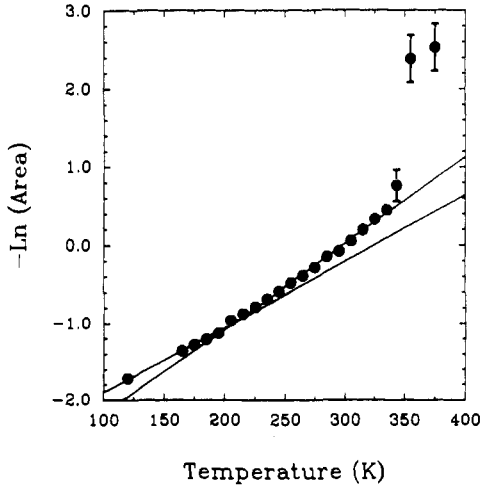

Figure 5. Plot of the natural logarithm of the normalized ^{57}Fe Mössbauer spectral area for $[Fe(C_5H_5)_2]PF_6$ versus temperature.

−ln (area) versus temperature behavior reflecting a change in the vibrational nature of the lattice. The data shown in Figure 5 show two breaks with increasing temperature which coincide with the two transitions seen in the heat capacity results for **1**. The ln (area) data collected in the low-temperature phase IV ($T <$ 211 K) and phase II (213 K $< T <$ 347 K) were fit to linear relationships and indicate Debye temperatures of 126 and 110 K, respectively. As expected, phase IV has the higher Debye temperature, indicating stronger lattice forces are present in this phase. The data in Figure 5 also show a large discontinuity between 343 and 355 K which corresponds to the temperature of the 347 K phase transition. The recoilless fraction of the high-temperature phase is considerably less than that of phase II. Thus, as is often the case, an order–disorder phase transition "softens" the lattice, decreasing the number of recoilless events, which is reflected in the corresponding ^{57}Fe Mössbauer spectrum as a decrease in spectral intensity. This "softening" associated with a phase change has been seen for other iron metallocene salts.[26] The limit of this behaviour is, of course, the solid to liquid phase change for which one would expect to see the ^{57}Fe Mössbauer spectrum vanish upon melting.

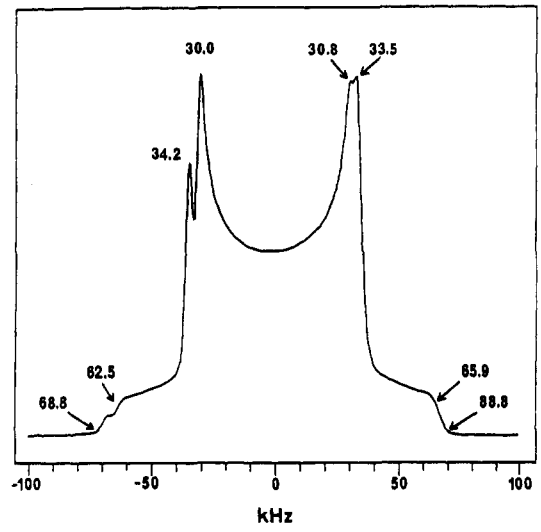

Figure 6. Solid-state ^{2}H NMR spectrum of $[Fe(C_5D_5)_2]PF_6$ at 286 K. Approximate values for the perpendicular and parallel edges of the two superimposed axial powder patterns are marked on the figure.

Solid-State ^{2}H NMR Spectroscopy. Variable-temperature solid-state ^{2}H NMR spectra were collected from 185 to 355 K for a polycrystalline sample of $[Fe(C_5D_5)_2]PF_6$. The room-temperature spectrum (Figure 6) is clearly the superposition of two axially symmetric powder patterns, each showing paramagnetic shifts no more than a few percent of the magnitude of the residual quadrupole couplings which dominate the pattern shape. The appearance of two resolved patterns is understandable, since there are two crystallographically different ferrocenium cations in the unit cell of the 299 K structure. Determination of the quadrupole couplings and paramagnetic shifts from single-crystal spectra with resolved doublets has been described previously.[10] In the case of powder spectra, we estimate these parameters as follows: since the paramagnetic shifts are only a few percent of the quadrupole couplings, we associate the apparent perpendicular and parallel edges in these spectra with the corresponding doublets one would observe in single-crystal spectra. This assumption is acceptable and the attendant error will be no more than the paramagnetic shifts. Furthermore, since the two lines of a given doublet are always paramagnetically shifted in the same direction, edges at positive and negative frequencies were paired in this way as well. The quadrupole couplings determined in this way were found to be twice as large for the parallel edges as for the perpendicular edges, as required for axial patterns. Applied to the room-temperature spectrum (Figure 6), this procedure gives a quadrupole coupling of 64 (2) kHz for both powder patterns.

The temperature dependence of the ^{2}H NMR spectra for a polycrystalline sample of $[Fe(C_5D_5)_2]PF_6$ is shown in Figure 7.

(26) Fitzsimmons, B. W.; Hume, A. R. *J. Chem. Soc., Dalton Trans.* **1980**, 180.

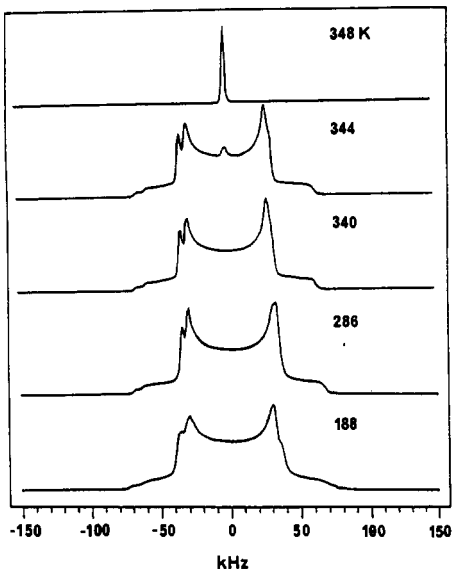

Figure 7. Variable-temperature solid-state ^2H NMR spectra of $[Fe(C_5D_5)_2]PF_6$.

Residual quadrupole couplings for the cyclopentadienyl rings are 67 (2), 64 (2), and 62 (2) kHz at temperatures of 188, 286, and 340 K, respectively. Static aromatic deuterons typically show quadrupole couplings, $(3/4)e^2qQ/h$, of 135–140 kHz and half that value at higher temperatures, where rapid in-plane ring reorientation in the solid-state occurs. Thus, the observed coupling at 188 K indicates rapid reorientation of both C_5D_5 rings about their local C_5 axes and, in addition, at higher temperatures some small-amplitude reorientation of the molecular axis as well. The root-mean-square amplitude of this libration is readily determined as 7° at 286 K and 10° at 340 K by the degree to which the coupling is decreased from the low-temperature limit. The libration has at least 3-fold symmetry in order to maintain the axial symmetry observed in the spectra.

At the 347 K phase transition, the 62-kHz splitting is abruptly and rigorously reduced to zero (the small spectral line width of 2 kHz requires that the residual coupling be less than 1 kHz). Since for all temperatures examined the C_5D_5 rings undergo rapid in-plane rotation, the observed abrupt collapse in quadrupole splitting is a reflection of the reorientation of the molecular axis. Consequently, in the high-temperature phase above 347 K the ^2H NMR results show that the reorientation of the ferrocenium cation approaches isotropic dynamics. Given the cubic symmetry of the high-temperature structure, the nominal picture of the dynamic disorder which averages the quadrupolar coupling (second-rank tensor interaction) to zero is a 3-fold jump among mutually orthogonal directions which is substantially less disorder than isotropic reorientation. Clearly, rapid ($\tau_c \ll 10^{-5}$ s) jumping among the 12 orientations identified in the proposed 360 K structure is consistent with the NMR results. Furthermore, the four-site precession about each axis could be regarded as an elaboration of the libration seen at temperatures below 347 K.

Within experimental resolution, the two room-temperature powder patterns show equivalent quadrupolar couplings; thus the resolution of the two deuteron types results from differences in paramagnetic shifts. Examination of the X-ray structure (Figure 2) shows that both inter- and intramolecular contributions to the shifts are likely. As determined from the perpendicular edges, paramagnetic shifts of −1.5 and 3.0 kHz are observed for the two well-resolved powder patterns at 340 K. The shifts increase to −2.0 and 3.5 kHz at 286 K. In this temperature range the appearance of two axial powder patterns is expected, since the unit cell contains two nonequivalent ferrocenium ions. At 188 K, the ^2H NMR spectrum does not have the degree of resolution observed at higher temperatures. Loss in resolution could arise from paramagnetic or exchange broadening or increased spectral complexity due to the possibility of more overlapping peaks with different paramagnetic shifts. Paramagnetic shifts in the range −2.0 to +5.5 kHz can be estimated. Thus, the paramagnetic shifts are relatively small and show the expected increase as the temperature is lowered. Little or no shift (<0.5 kHz) is observed for the isotropic line in the high-temperature phase.

It is important to note that the ^2H NMR studies of these paramagnetic solids are greatly facilitated by extremely rapid electron longitudinal relaxation rates. By inversion recovery methods, T_1 values were estimated to be 2, 6, 9, and 14 ms for relaxation of the perpendicular edge signals at temperatures of 188, 286, 340, and 360 K, respectively. Relaxation of the parallel-edge signals ($T < 347$ K) is typically about half as long as that for the perpendicular-edge signals. The minimum relaxation time expected for a planar reorientating cyclopentadienyl deuteron due only to quadrupolar relaxation time of $T_1 = 2.2$ ms ($\tau_c = 1$)[27] is slightly larger than the minimum value of 2 ms observed here, and thus we conclude that an additional relaxation mechanism, namely paramagnetic relaxation, is operative as well. Since no substantial change in the relaxation time accompanies the phase transition at 347 K, where there is a dramatic change in the molecular dynamics, paramagnetic relaxation is likely the dominant mode. Furthermore, since the quadrupole spectral features are well-resolved at all temperatures and T_1 increases with temperature, the relevant correlation time is always short ($\tau_c \ll 1$). Probably the electronic relaxation time, T_{1e}, rather than the correlation time for the C_5D_5 in-plane rotation determines the relaxation rate.

Solid-state ^2H NMR studies on a variety of paramagnetic complexes should be feasible. NMR of paramagnetic solids is substantially less restrictive than that in liquids since the interactions are typically about 3 orders of magnitude larger (quadrupolar couplings in solids are about 100 kHz versus chemical shifts in liquids of about 100 Hz for ^1H and ^2H NMR spectra).

Microscopic Model for the Orientational Motions Experienced in the Plastic Phase of $[Fe(C_5H_5)_2]PF_6$. With the extensive amount of crystallographic and spectroscopic information known about **1**, it seems reasonable to attempt to construct a model of the orientational motions experienced by the cations and the anions in the high-temperature plastic phase which is in keeping with the observed thermodynamics of the 347 K phase change. Often, models which attempt to account for the microscopic motion which sets in at an order–disorder phase transition are proposed and subsequently confirmed on the basis of how well the theoretical entropy of transition, ΔS, matches the experimentally observed value.[28] In the theoretical entropy calculations, it is assumed that, for an order–disorder phase transition, the total entropy change for a transition can be approximated by summing a term $R \ln (N_2/N_1)$ for each of the constituents (i.e., anion and cation) of the solid that become disordered from N_1 distinguishable orientations to N_2 distinguishable orientations. Credence is lent to this type of treatment because experimentally determined entropy values cluster around small integer numbers such as $R \ln N$, where $N = 2, 3, 4$, etc.[28]

However, the addition of entropy change contributions to give a total entropy change for an order–disorder phase transition is only strictly valid when the component parts, such as the anion and cation, act independently. If this is *not* the case, and there is some concerted (i.e., coupled) orientational motions of the components present in a solid, the entropy gain cannot simply be calculated by adding together entropy gains associated with the various molecular constituents. This phenomenon where disor-

(27) Torchia, D. A.; Szabo, A. *J. Magn. Reson.* **1982**, *49*, 107.
(28) Parsonage, N. G.; Staveley, L. A. K. *Disorder in Crystals*; Claredon Press: Oxford, England, 1978.

dered populations interfere with one another is known as frustration. Parsonage and Staveley realized that calculating the transition entropy for a solid composed of interfering polyatomic components would be extremely complex.[28] They noted that a "solid without [a] passive 'diluent' would be in a disordered state for which the entropy could only be calculated with great difficulty". A theoretical model which encompasses the extent of correlation of the orientational motions of the different constituents is necessary to explain the experimentally observed entropy gain. In the following discussion, we first examine the thermodynamic considerations of a model of orientational motion for a simple two-component system in which correlated motion occurs. Then, we use these same considerations to construct a model of the motions experienced in the high-temperature plastic phase of $[Fe(C_5H_5)_2]PF_6$.

Consider a system that contains two components, A and B, each of which has one orientation in the lower temperature phase (phase I) and upon a phase transition is dynamically disordered in two orientations in the higher temperature phase (phase 2), viz.

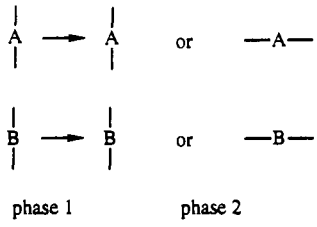

If the motions of A and B are not coupled, the transition entropy is expected to $\Delta S = k \ln (4/1)$ or $R \ln 4$ for 1 mol. If, however, the motion of B is coupled to that of A, e.g. for steric reasons, such that when A is horizontally aligned, B cannot also be horizontally aligned, this means that of the four theoretically possible microstates, only three are allowed because one has been excluded due to the coupling of the motion of B and A, viz.

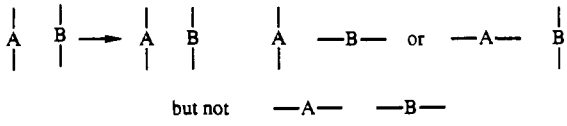

Since B's orientations are coupled to A's orientations, the number of possible microstates in the high-temperature phase has been reduced by 1. Therefore the observed transition entropy is reduced to give $\Delta S = \sum k \ln [(4-1)/1] = R \ln 3$. The coupled motion has reduced the transition entropy. This treatment implies that the total number of microstates, W_{tot}, of the unit cell can be calculated in both phases if one knows the number of excluded microstates, W_{excl}, of components A and B in phase 2 due to the coupling. Since B is coupled to A, the number of microstates for B (W_B) is reduced by the number of B coupled microstates (W_{excl}) to give $W_B = (W_{poss} - W_{excl})$. The number of coupled microstates that are excluded can be calculated if one knows the following: (1) the number of A orientations which exclude B orientations, X; (2) the total number of A orientations, X_{tot}; and (3) the number of B orientations excluded by an orientation of A, Y. Then W_{excl} is given by eq 3. In the above simple example this gives $W_B =$

$$W_{excl} = (X/X_{tot})Y \qquad (3)$$

$2 - (1/2)(1) = 3/2$ and, therefore, $W_{tot} = W_A W_B = (2)(3/2) = 3$ and $\Delta S = R \ln 3$.

However, extension of the coupling interactions to outside the unit cell leads to a different consideration. In the model system just considered, the coupling interactions were assumed localized in the unit cell. If this is not the case (i.e., not only are the orientations of B coupled with those of A but also the orientations of A are coupled to those of B), the coupling interactions extend to adjacent unit cells. Long-range correlation effects can reduce considerably the transition entropy, sometimes by as much as a factor of N, which for a macroscopic sample can be many orders of magnitude. Hence, the entropy gain for a completely correlated phase transition is predicted to be exceedingly small and therefore undetectable. For this reason, an observed order–disorder phase transition which exhibits a measurable thermal anomaly is most certainly due to an uncorrelated phase change; i.e., at least one component is not coupled.

Now consider the reorientational motions in the plastic phase of $[Fe(C_5H_5)_2]PF_6$. Below the 347 K phase transition, the ferrocenium cations are found to have four orientations in the unit cell and the solid-state ^2H NMR results indicate that the cations are static in their respective orientations. However, there are in actuality two possible cases: first, the cations could truly be static (i.e., reorientation rate is effectively zero), or second, the cation could be reorienting at a rate that is slow relative to the deuterium NMR time scale ($\sim 10^5$/s). There are two pieces of evidence that support the latter view. The quadrupole coupling is temperature dependent in phase II (213 K < T < 347 K), suggesting that the cations are reorienting and the rate of this process as well as the amplitude of the motion increases with increasing temperature.

At the 347 K phase transition, the ferrocenium cations become dynamically disordered, as evidenced by the reduction of the deuterium quadrupolar interaction to zero. There are twelve orientations in the proposed high-temperature crystal structure. The PF_6^- anions occupy only one crystallographic orientation in the 299 K structure and are disordered in four orientations in the 360 K structure. However, each PF_6^- anion spends less time in three of the orientations than in the fourth. We have no direct evidence whether or not the PF_6^- anions are dynamic between the four different lattice positions found in the 360 K structure. However, there are two indirect pieces of evidence for a dynamic disorder. Since there is a 4% increase in the volume of the unit cell at 347 K phase transition and the larger ferrocenium cation is clearly dynamic, it is very likely that the PF_6^- anion is dynamically reorienting. The second piece of evidence comes from preliminary results of a solid-state ^{19}F NMR study, which show that even at room temperature a narrow signal is seen, suggesting the PF_6^- anions are dynamic.

In $[Fe(C_5H_5)_2]PF_6$, the cation converts from four orientations in the room-temperature phase to twelve orientations in the high-temperature phase, while the PF_6^- anion converts from one orientation to four orientations. The simple theoretical transition entropy for this model can be estimated from the fact that in the room-temperature phase there are four possible microstates (one anion and four cation orientations) and in the high-temperature phase there are forty-eight microstates (four anion and twelve cation orientations). However, the transition entropy of $R \ln 12$ greatly exceeds the experimentally determined value of 13.99 J/(mol K) ($=R \ln 5.38$). Even if one considers that the PF_6^- anion microstates are unequally populated and therefore require a Boltzmann-weighted entropy gain,[28] the total transition entropy calculated, 17.49 J/(mol K) ($=R \ln 8.20$), is still appreciably larger than the experimental value.

Since both ions in $[Fe(C_5H_5)_2]PF_6$ are polyatomic and since the experimental transition entropy is appreciably less than the simple theoretical transition entropy value, it seems likely that there is orientational frustration present in this system. The nature of the coupled motion of the $[Fe(C_5H_5)_2]^+$ and PF_6^- ions was easily detected upon evaluating the contact distances of each cation and anion orientation in the proposed 360 K structure. It was found that the three 11% occupancy orientations of neighboring PF_6^- anions are excluded by nine of the twelve cation orientations. The space-filling drawing in Figure 8 shows the appreciable contact that develops between the cation and anion

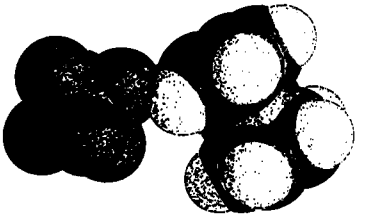

Figure 8. Space-filling plot showing the contact that develops between a $[Fe(C_5H_5)_2]^+$ cation and a nearby PF_6^- anion when the cation is in nine of its twelve orientations and the anion is in one of its three low-occupancy orientations in the phase above the 347 K first-order phase transition.

in one of these excluded orientations. Therefore, the coupling model is one in which three orientations of the PF_6^- anion are excluded by nine of the twelve orientations of the nearby cations due to steric constraints. Thus, it is found that for the anion $W_{excl} = (9/12)(3) = 9/4$ and $W_B = 4 - (9/4) = 7/4$. This gives for the number of orientations above 347 K a value of $W_2 = W_A W_B = (12)(7/4) = 21$ and below 347 K a value of $W_1 = 4$. Therefore, the transition entropy is found to be $\Delta S = k\sum \ln W_2/W_1 = R \ln 5.25$, unless the coupling interactions are extended to outside the unit cell. This agrees with the observed transition entropy value of $R \ln 5.38$. However, it should be remarked that the observed transition entropy depends upon how the normal heat capacity curves (i.e., the baselines) have been estimated. The experimental value,[8] $\Delta S = R \ln 5.38 = 13.99$ J/(mol K), has been obtained on the basis of two baselines determined independently for the temperature regions below and above 347 K. If a single baseline connecting smoothly the whole temperature region were adopted, the observed entropy would be by ~1 J/(mol K) larger than 13.99 J/(mol K).

At any rate, the excellent agreement between the experimental and calculated transition entropy values for $[Fe(C_5H_5)_2]PF_6$ lends credence to this theoretical method of estimating entropy gains for order–disorder phase transitions involving coupled component motion. In fact, $[Fe(C_5H_5)_2]PF_6$ in its complexity proves to be the prototypical system for which this method should work the best. Other systems with polyatomic component exist which also do not have $\Delta S = R \ln N$ values where N is some integer. If these were reexamined with the above considerations in mind, the ΔS values for the order–disorder phase transitions in these systems might also be explained.

At this point, a consideration of other possible space groups for the 360 K structure is warranted. If the structure actually exists in $Pm\bar{3}m$ and not $Pm\bar{3}$, the number of cation orientations increases to 24 due to the additional symmetry element. However, the number of excluded orientations also increases by a factor of 2. Thus $W_{excl} = (18/24)(3) = 9/4$, and hence the arguments presented above are still valid. In this case, the thermodynamic results are consistent for both $Pm\bar{3}$ and $Pm\bar{3}m$ structures.

Conclusions

Examination of the 347 K first-order phase transition of ferrocenium hexafluorophosphate by means of X-ray diffraction, both single crystal and powder, and solid-state ^2H NMR and ^{57}Fe Mössbauer spectroscopies indicates that this phase transition involves disordering motion of both the $[Fe(C_5H_5)_2]^+$ cations and the PF_6^- anions. It was shown that the ferrocenium cation changes from four orientations below the phase transition to being dynamically disordered in twelve equal energy orientations above the phase transition. The PF_6^- anion goes from one orientation to being dynamically disordered in four non-equal-energy orientations. A theoretical model was presented to explain the entropy gain determined in heat capacity measurements. The results for the 360 K X-ray structure show that when the ferrocenium cation is in nine out of twelve of its orientations, it excludes the nearby PF_6^- anions from being in three of their four orientations. A statistical mechanical model for this coupled motion of anion and cation predicts $\Delta S = R \ln 5.25$, in good agreement with the experimental value of $R \ln 5.38$.

Acknowledgment. We are grateful for support from National Institutes of Health Grant HL-13642 (D.N.H.) and National Science Foundation Grant DMB-86-06358 (R.J.W.). M.S. and D.N.H. are also grateful for a travel grant (INT-9016821) from the National Science Foundation and the Japan Society for the Promotion of Science.

Supplementary Material Available: Tables giving crystal data and details of the structure determination, atomic thermal parameters, and calculated hydrogen atom positional parameters for the 299 and 360 K X-ray structures of $[Fe(C_5H_5)_2]PF_6$ (5 pages). Ordering information is given on any current masthead page.

Registry No. Ferrocenium hexafluorophosphate, 11077-24-0.